ORIGIN OF NANOPARTICLE NUCLEI: FORMATION OF DIMERS IN PULSE MAGNETRON DISCHARGES

[1]Pavel CURDA, [2,3]Rainer HIPPLER, [2]Martin CADA, [1]Vitezslav STRANAK, [2]Zdenek HUBICKA

[1]University of South Bohemia, Faculty of Science, Ceske Budejovice, Czech Republic, EU, pcurda@jcu.cz

[2]Institute of Physics, Czech Academy of Sciences, Prague, Czech Republic, EU

[3]University of Greifswald, Greifswald, Germany, EU

https://doi.org/10.37904/nanocon.2023.4763

Abstract

The study focuses on the synthesis of metallic nanoparticles (NPs) by gas aggregation of magnetron sputtered atoms. Such NPs have gained significant attention because of their wide potential applications. For that reason, the cost-efficient and energy-effective synthesis of NPs is wanted. The growth of NPs follows processes of dimer seed nucleation, atom adsorption, and coagulation; the initial nucleation of the seed, i.e., dimer origin, is considered the most limiting part of growth. Hence, it is believed, that if dimer seeds are produced effectively, the NPs growth will follow this trend, too.

Various pathways exist for the synthesis of diatomic molecules in magnetron sputtering. The three-body collision reactions, involving two metal and one gas atom M+M+G, suffer from relatively low reaction coefficients indicating practically negligible contribution of this reaction to dimer production. Two-body collision reactions, driven by ionization events and electron release, have gained significance due to their higher rate coefficients. However, direct sputtering of metal dimers from the target material offers straight forward and effective way that yields the highest and direct production of dimers M_2. This study investigates pulsed magnetron discharges, namely the pulse repetition frequency and the pulse width, to reveal the optimal conditions for direct dimer sputtering. The dimer sputtering efficiency is estimated from energy-resolved mass spectroscopy measurements. Overall, this study underscores the significance of fine-tuning production processes for diatomic molecules, offering a pathway to advanced nanoparticle synthesis.

Keywords: Dimer, nanoparticle, gas aggregation synthesis, magnetron sputtering, energy-resolved mass spectrometry

1. INTRODUCTION

Over recent decades, metallic nanoparticles (NPs), objects with dimensions in the order of tens of nanometers, have drawn attention due to their wide application potential including optics [1], electronics [2], catalysis, biomedicine or (bio)sensing [3] and many others. For that reason, the industry seeks for optimization of the NPs production in terms of cost, energy, and time efficiency. Gas aggregation of magnetron sputtered atoms at elevated pressure [4] is one of the methods utilized for nanoparticle production. The concept, originally proposed by H. Haberland et al [5], namely benefits from high purity process and possible deposition of NPs onto (planar) substrates making e.g., platforms for sensing structures. The process is characterized by atom evaporation of a target material and subsequent condensation of free metal atoms of supersaturated vapor, through thermalizing collisions, into nanoparticles. The growth process can be divided into three steps: seed nucleation, atom adsorption, and coagulation [6]. It is the initial formation of the seed nucleus that is considered a bottleneck for efficient nanoparticle production [5]. On the other hand, the other two growth steps, atom adsorption, and coagulation are rather quick processes.

The stable nuclei must fulfill the thermodynamic equation

$$r_c = \frac{2 \cdot \sigma \cdot m}{k \cdot T \cdot \rho \cdot \ln \phi_k}, \quad (1)$$

where r_c is the critical radius, σ is the surface tension, ρ denotes material density, m represents the mass of the nuclei, k stands for Boltzmann constant, T is the temperature in the aggregation region and ϕ_k is the ratio between vapor pressure and saturation vapor pressure [7]. Under realistic experimental conditions present in a gas aggregation nanoparticle source, the smallest species that fulfills equation (1) is a diatomic molecule. Hence, the goal of the cost and energy-efficient synthesis lies in the optimized production of dimer molecules [7]; in other words, these are dimers, acting as necessary seeds for the further growth of NPs.

There are multiple paths for the synthesis of diatomic molecules in magnetron sputtering. The first one is the three-body collision of metal atoms with a gas species M + M + Ar → M_2 + Ar; the Ar is typically employed as a process gas in the aggregation systems. Another possible channel for dimer production is the propagation of argon dimer by Ar^+ + Ar + Ar → Ar_2^+ + Ar, and lastly combined molecule by Ar^+ + Ar + M → ArM^+ + Ar. All the above-mentioned reactions suffer from very low reaction coefficients and nowadays are considered rather negligible contributors to dimer production [5]. Another path for the synthesis of diatomic molecules in the gas phase is by two-body collisions. Here ionization must occur, to produce free electrons that enable the conservation of momentum. One example of such a reaction is Ar^{**} + Ar → Ar_2^+ + e, where Ar^{**} denotes a highly excited Ar atom. While the population of Ar^{**} is generally smaller than the population of Ar^+ in magnetron discharges, the rate coefficient of two-body collision is much larger, which makes the two-body collision a possible contributor to Ar_2 dimer production [8]. The second channel for dimer production is Ar^* + M → ArM^+ + e. Here the ionization energy of metal must be smaller than the first metastable state of Ar^* which lies at 11.5 eV [9]. This condition is fulfilled for many transition metals commonly used for nanoparticle synthesis. The third option of dimer production is a direct sputtering of metal dimers from the target as shown in [10]. This paper focuses on the optimization of magnetron parameters for efficient sputtering of dimers directly from the target. For that reason, the pulsed magnetron discharges are investigated, and the role of the pulse repetition frequency and the pulse width are evaluated. Furthermore, the optimization of magnetron properties can help to encourage the synthesis of gaseous dimers, too.

2. MATERIAL AND METHODS

The utilized experimental configuration enables magnetron operation in a pulsed regime. The energy-resolved mass spectrometer was employed to detect and specify the species sputtered from the target.

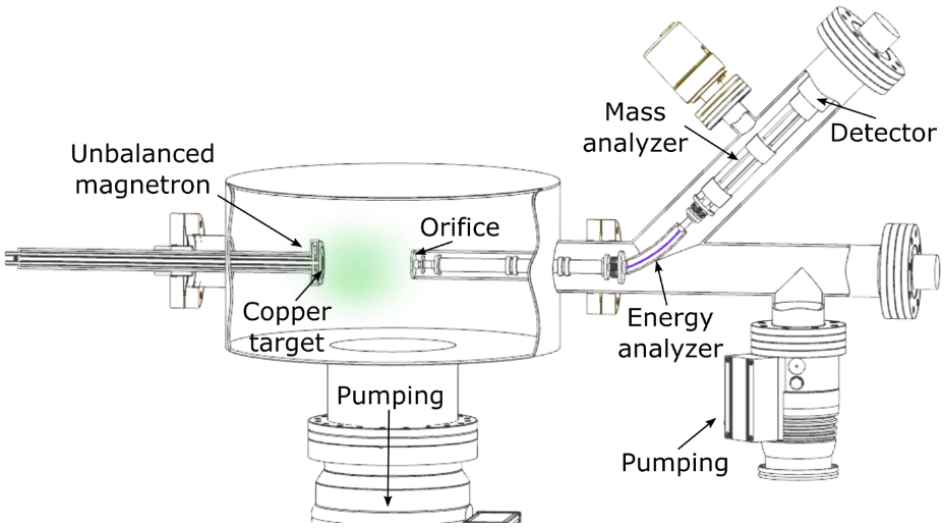

Figure 1 Experimental setup with unbalanced sputtering magnetron equipped by Cu target facing towards mass/energy analyzer orifice with distance 140 mm.

For that reason, the spectrometer orifice was directly facing the sputtered cathode (Cu target) of a magnetron gun, see **Figure 1**. A commercial (Kurt J. Lesker, Torus) planar unbalanced magnetron with a copper target (diameter 50 mm, thickness 6 mm, purity 99.7 %) was mounted sidewise into a vacuum chamber. Process gas (Ar) is introduced to the vacuum chamber by a mass flow controller with a flow rate of 80 sccm. A valve installed between the vacuum chamber and the turbomolecular vacuum pump allowed to keep the pressure, measured by a capacitance vacuum gauge, at 1 Pa for all experiments. The cathode voltage is delivered by a DC power supply (Advanced Energy MDX-500) serially connected with a home-built power switch and a ballast resistor [11]. The repetition frequency was set to 1,000 Hz for all experiments, while the pulse width was varied T_a = 20 - 280 µs, using the two-channel arbitrary waveform generator (OWON AG 1022). Voltage and current waveforms were simultaneously monitored using voltage (Agilent 10076 A) and current probes (Textronix A622), respectively, both connected to a two-channel digital oscilloscope (Agilent DSO 6012A). Hiden EQP 1000 mass/energy analyzer (Hiden Analytical Ltd., UK) [12] was employed for the detection of Cu^+, Ar_2^+, $ArCu^+$, and Cu_2^+. The spectrometer orifice was mounted opposite from the magnetron at 140 mm just facing the target.

3. RESULTS AND DISCUSSION

The magnetron was operated in a pulse regime; the voltage and current waveforms for different pulse widths are shown in **Figure 2**. To keep the same energy of argon ions impinging the target surface, the voltage was kept at a constant value of -480 V concerning the ground. Because the pulse repetition frequency was kept constant (f = 1,000 Hz) the average power P_p calculated as

$$P_p = \frac{1}{T} \cdot \int_0^T U(t) \cdot I(t) \cdot dt, \tag{2}$$

results in P_p = 16, 53, 98, 181, and 245 W respectively. The negative voltage appears rather quickly onto the cathode and only slightly increases after the pulse rises. The behavior of the current follows qualitatively the same trend, with an observable delay of the rising characteristics, see **Figure 2**. The current decreases after peaking which might be attributed to the sputtering wing effect [13].

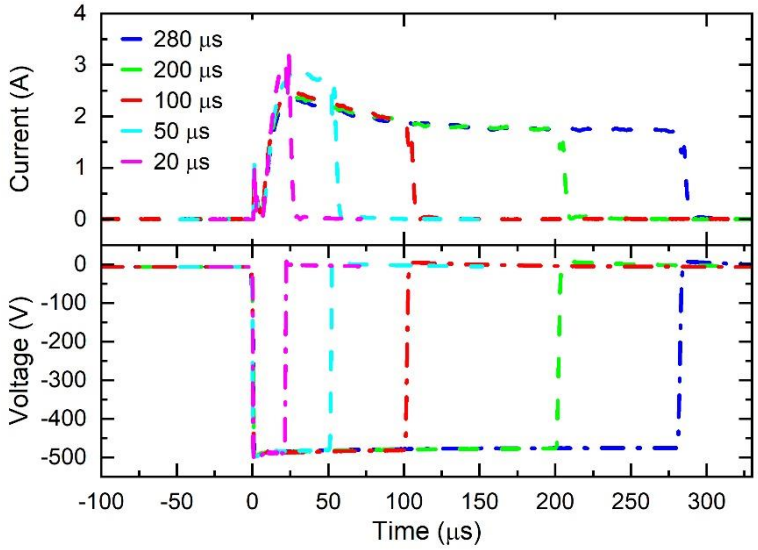

Figure 2 The current (upper panel) and the voltage (bottom panel) waveforms were measured for discharges with pulse widths of 20, 50, 100, 200, and 280 µs, respectively. The pulse repetition frequency was kept constant for all experiments (1,000 Hz) as well as the voltage (-480 V).

The production of ionized dimers in pulsed discharge will be discussed for Cu_2^+, $ArCu^+$, and Ar_2^+, whose signal was measured by mass spectrometry. Similar behavior for their neutrals is expected since the ionization takes

place near the cathode region where the electron density is large and ionization probabilities are high [14]. It is expected that the sputtered species leave the target as neutrals are subsequently ionized in the discharge.

Figure 3 left panel shows the energy spectra measured for Cu_2^+ for discharges operated with pulse widths 20, 100, and 280 μs. The count rate was normalized to power, which allowed the comparison of the production efficiency of investigated dimers. All distribution bodies show qualitatively similar behavior. The distribution body stretches to energies of up to 35 eV, which are received from the direct sputtering. Well pronounced low energy peak, around 3-5 eV, is most probably a result of thermalizing collisions of metal species with Ar atoms that can occur in the plasma bulk. It is also worth noting that the intensity of the thermalized peak stretches to higher values for more energetic discharges that are operated with shorter pulse widths (20 μs). **Figure 3** right panel compares energy distributions for Cu^+, Ar_2^+, $ArCu^+$, and Cu_2^+, respectively, measured in discharge with the pulse width T_a = 100 μs. Single copper ion Cu^+ displays Thompson's high energy tail similar to Cu_2^+; a typical feature of magnetron sputtered species. However, single ion Cu^+ attains energy levels as high as 100 electron volts (eV), whereas the range of energy for copper dimers Cu_2^+ is limited to approximately 35 eV, see **Figure 3**. Taking the mass ratio Cu^+/Cu_2^+, one could anticipate energies of up to 50 eV for larger dimers [15]. Higher measured values are attributed to increased energy dissipation during the transport phase in an argon gas environment at 1 Pa. The other two species, $ArCu^+$ and Ar_2^+, are most likely products of gaseous reactions, as none of these dimers showcase the high-energy tail. The qualitatively similar behavior was observed for all conditions, with maximum intensity being changed.

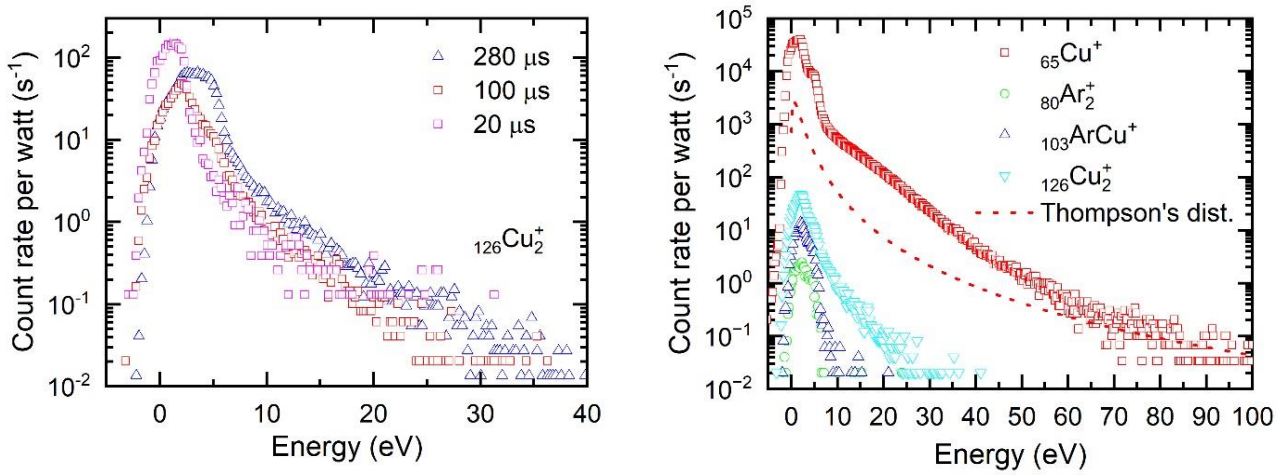

Figure 3 Left: Energy distribution of $_{126}Cu_2^+$ ions for different pulse widths; the high energy tails follow the Thompson distribution. Right: Energy distributions for $_{65}Cu^+$, $_{80}Ar_2^+$, $_{103}ArCu^+$, and $_{126}Cu_2^+$ ions measured in the discharge operated with the pulse width 100 μs. The count rates are normalized to the unit of power.

To evaluate the energy efficiency of a dimer production the integrated intensity of measured signal per power unit was calculated according to

$$I = \frac{\int_{e_1}^{e_2} N(E,t)dE}{P_p}, \quad (3)$$

where N denotes count rate, e_1 and e_2 represent the measured energy rates, dE is the energy step and P_p stands for average power. The results for Cu^+, Ar_2^+, $ArCu^+$, and Cu_2^+ with the integrated intensities are presented in **Figure 4.** The copper ion intensity, which is the highest for all measured ions, exponentially (i.e., linearly in a semilogarithmic scale) decreases with increasing the pulse width.

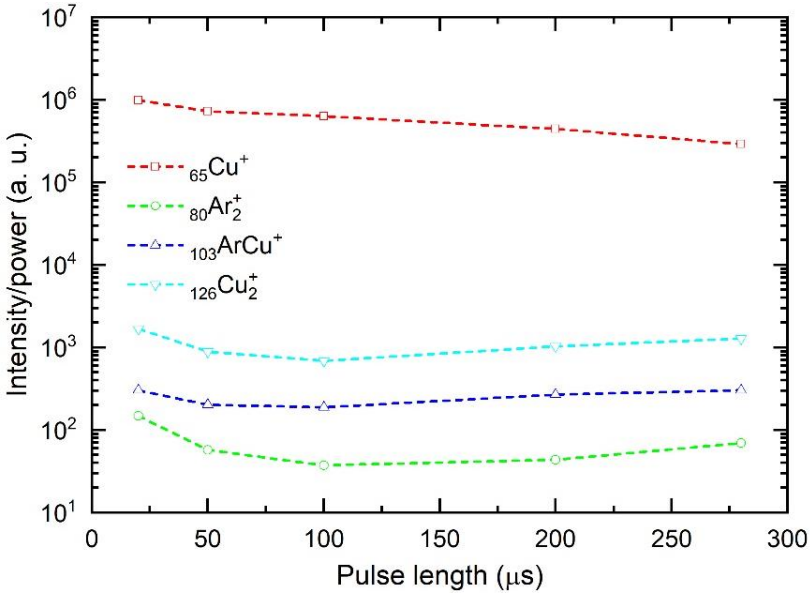

Figure 4 The integrated ion intensity divided by average power (representing a number of arriving ions) as a function of the pulse width measured for $_{65}Cu^+$, $_{80}Ar_2^+$, $_{103}ArCu^+$, and $_{126}Cu_2^+$. The pulse repetition frequency (f = 1,000 Hz) and the cathode voltage (-480 V) were kept constant for all measurements.

This behavior is attributed to changes in the instant discharge power. Since the pulse width increases but the pulse frequency stays constant the duty cycle increases, too. The highest production appears at low pulse width, i.e., low duty cycles, where the energy is accumulated into the short pulse which enhances the ionization degree of sputtered metal atoms which increases the Cu^+ ion population [16,17]. However, both Cu and Cu^+ are not of significant interest for dimer formation since the M + M + Ar → M_2 + Ar reaction is slow and improbable, see above. On the other hand, the objects of our interest, dimers, behave differently: the highest intensity is observed at pulse width T_a = 20 μs, the population then decreases until about T_a = 100 μs and then rises again, see **Figure 4**. Such a trend is observed for all investigated dimers (Cu^+, Ar_2^+, $ArCu^+$, and Cu_2^+). The highest intensity among the dimers was measured for Cu_2^+, which is about one order of magnitude higher than $ArCu^+$ and even two orders of magnitude higher than Ar_2^+; see **Figure 4**. Here, let us remind you that Cu^+ and Cu_2^+ species are considered as directly sputtered from the target, as indicated by their Thompson distributions shown in **Figure 3**, while the origin of those Ar_2^+, $ArCu^+$ dimers is expected in gas synthesis channel that is ineffective. Hence, this supports the idea that these are directly sputtered dimers (Cu_2^+ in our case) which play a key role in nanoparticle production. of nanoparticle nuclei and the most energy efficient conditions for Cu_2^+ production were found at T_a = 20 μs.

4. CONCLUSION

This study focuses on the investigation of metal dimers directly sputtered from the target; in our model situation, Cu_2^+ dimers were studied. It is believed that directly sputtered dimers play a key role in nanoparticle production in gas aggregated systems because they serve as an elemental nucleus (seeds) initiating NPs growth by subsequent atom adsorption. Since the population of Cu_2^+ species has the Thompson energy distribution, it is believed that these dimers are directly sputtered from the target. The dimer population is lower by about several orders of magnitude if compared with single Cu^+ atoms but is still significantly higher than the population of Ar_2^+ and $ArCu^+$ that originate through ineffective gas synthesis reactions. The directly sputtered dimer production can be maintained by pulsed magnetron discharges. It was shown that the pulse width (and the duty cycle) influences the sputtered dimers population that was found the highest at low duty cycles (T_a = 20 μs, f = 1,000 Hz) when the instantaneous power density is high. These findings highlight the importance of optimizing Cu_2^+ production conditions.

ACKNOWLEDGEMENTS

The research was financially supported by the Czech Science Foundation through the project GACR 21-05030K and by the Ministry of Education, Youth and Sports of the Czech Republic through the project "Solid state physics for the 21st century" CZ.02.1.01/0.0/0.0/16_019/0000760.

REFERENCES

[1] FLORY, F., ESCOUBAS, L., ROUZO, J. et al. Low-dimensional optics. *Journal of Nanophotonics*. 2015, vol. 9, no. 1, 093594.

[2] LIU, Y., ZHANG, J., PENG, L.M. Three-dimensional integration of plasmonics and nanoelectronics. *Nature Electronics*. 2018, vol. 1, pp. 644-651.

[3] YING, Y.L., HU, Y.L., ZHANG, S. et al. Nanopore-based technologies beyond DNA sequencing. *Nat. Nanotechnol*. 2022, vol. 17, pp. 1136-1146.

[4] GRAMMATIKOPOULOS, P., STEINHAUER, S., VERNIERES, J. et al. Nanoparticle design by gas-phase synthesis. *Advances in Physics*: *X 1:1*. 2016, pp. 81-100.

[5] HABERLAND, H., ISSENDORFF, B., KOLAR, T. et al. Electronic and geometric structure of Ar n+ and Xe n+ clusters: The solvation of rare-gas ions by their parent atoms. *Phys. Rev. Lett*. 1991, vol. 67, 3290.

[6] HUTTEL Y. Gas-Phase Synthesis of Nanoparticles. *John Wiley & Sons*. 2017.

[7] KASHTANOV, P.V., SMIRNOV, B.M., HIPPLER, R. Magnetron plasma and nanotechnology. *Physics-Uspekhi*. 2007, vol. 50, pp. 455-488.

[8] BOGAERTS, A., GIJBELS, R. Role of Ar 2+ and Ar 2+ ions in a direct current argon glow discharge: A numerical description. *Journal of Applied Physics*. 1999, vol. 86, pp. 4124-4133.

[9] BALLOU, J. K., LIN, C. C., FAJEN, F. E. Electron-impact excitation of the argon atom. *Physical Review A*. 1973, vol. 8, no. 4, 1797.

[10] CURDA, P., HIPPLER, R., CADA, M. et al. The role of dimers in the efficient growth of nanoparticles. *Surface and Coatings Technology*. 2023, vol. 473, 130045.

[11] STRANAK, V., DRACHE, S., CADA, M. et al. Time-Resolved Diagnostics of Dual High Power Impulse Magnetron Sputtering With Pulse Delays of 15 μs and 500 μs. *Contrib. Plasma Phys*. 2011, vol. 51, pp. 237-245.

[12] TOLSTOGOUZOV, A., DAOLIO, S., PAGURA C. et al. Energy distributions of secondary ions sputtered from aluminum and magnesium by Ne+, Ar+ and O2+: a comprehensive study. *Intern. J. Mass Spectrom*. 2002, vol. 224, pp. 327-337.

[13] GUDMUNDSSON, J. T., BRENNING, N., LUNDIN, D. et al. High power impulse magnetron sputtering discharge. *Journal of Vacuum Science & Technology A*. 2012, vol. 30, no. 3.

[14] S. ROSSNAGEL, S. Ionization by radio frequency inductively coupled plasma. Thin Films. 2000, 27, 37-66.

[15] HIPPLER, R., DENKER, C. Formation of (),(n= 1, 2), and ArCu+ ions during sputtering of a copper surface by low-energy Ar+ ion bombardment in a dilute argon atmosphere. *Plasma Sources Sci. Technol*. 2018, vol. 27, 065010.

[16] VLČEK, J., KUDLÁČEK, P., K. BURCALOVÁ, K. et al. Ion flux characteristics in high-power pulsed magnetron sputtering discharges. *EPL*. 2007, vol. 77, 45002

[17] ROSSNAGEL, S.M., HOPWOOD, J. Magnetron sputter deposition with high levels of metal ionization. *Appl. Phys. Lett*. 1993, vol. 13, pp. 3285-3287.